THE JOURNAL OF PHYSICAL CHEMISTRY B

Article

pubs.acs.org/JPCB

Effect of Axial Ligand on the Binding Mode of M-*meso*-Tetrakis(*N*-methylpyridinium-4-yl)porphyrin to DNA Probed by Circular and Linear Dichroism Spectroscopies

Lindan Gong,[†] Inho Bae,[‡] and Seog K. Kim[†,*]

[†]Department of Chemistry, and [‡]Department of Physics, Yeungnam University Gyeongsan City, Gyeong-buk, 712-749 Republic of Korea

ABSTRACT: The binding modes of cationic porphyrins, namely M-*meso*-tetrakis(*N*-methylpyridinium-4-yl)porphyrin (MTMPyP, where M = free base, Cu(II), Ni(II), Co(III), Mn(III), V(IV)═O, and Ti(IV)═O), to native DNA were systematically investigated by polarized light spectroscopies, viz. circular and linear dichroism spectroscopy (CD and LD, respectively). At low [porphyrin]/[DNA] ratio, planar porphyrins including TMPyP, CuTMPyP, and NiTMPyP exhibited a negative CD signal in the Soret region and large negative wavelength-dependent LD^r signal which is characteristics of their intercalative binding mode. In the intercalation pocket, the molecular plane of porphyrin is skewed to a large extent as it was judged from a large wavelength-dependency of the LD^r magnitude in the Soret region. As the mixing ratio was increased, a bisignate CD spectrum became apparent for all of the planar porphyrins, while the shape of LD^r remained the same, indicating the coupling of the electric transition moments of the intercalated porphyrins. Thus, coupling can occur between the porphyrins when they are separated at least two DNA base-pairs according to the nearest neighboring site exclusion model. This coupling interaction was the weakest for NiTMPyP. The porphyrins with axial ligands, namely VOTMPyP, TiOTMPyP, MnTMPyP, and CoTMPyP, bind to the exterior of the DNA at a low [porphyrin]/[DNA] ratio, which is indicated by the positive CD signal in the Soret region. The absorption and LD spectra in the Soret region were treated as the sum of two transitions to calculate the angle between each of the electric transition moments of the porphyrin, i.e., the B_x and B_y transitions relative to the local DNA helix axis. The angle of one of the two electric transitions of the porphyrin is in the range of 56°∼59°, whereas the other is in the range of 59°∼65°. Increasing the porphyrin density resulted in the appearance of an interaction between the bound porphyrins, which was indicated by the distorted CD spectra. In contrast with the planar porphyrins, which are parallel to each other in the intercalation pocket when they interact by themselves, the molecular plane of the porphyrin with the axial ligand tilts more toward the local DNA helix axis as the population of porphyrins was increased. CoTMPyP exhibited complicated CD and LD spectra at high [porphyrin]/[DNA] ratios that were impossible to explain by the presence of two porphyrin species: those with a monomeric external binding and electric coupling. Since the CoTMPyP−DNA complex started to aggregate at relatively low [porphyrin]/[DNA] ratios, the complication may due to the involvement of extensive porphyrin aggregation.

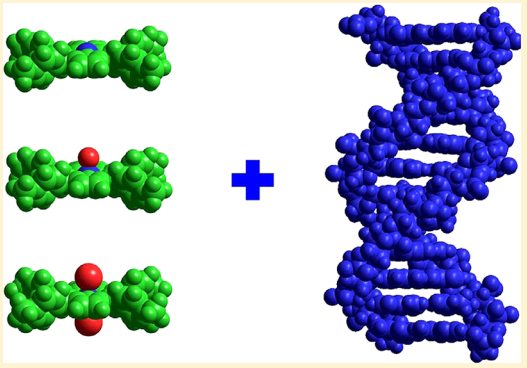

INTRODUCTION

Following the pioneering work of Pasternack[1] and Fiel,[2] the binding of cationic porphyrins to DNA has been widely studied, due to their potential application in medicinal chemistry and biology.[3−10] Several binding modes to native and synthetic double stranded DNA, which are affected by a variety of factors including the structure of the periphery groups, the number and position of the positive charges, and the nature of DNA have been identified, including intercalation between DNA base-pairs,[11−13] grooving binding,[13−20] outside random binding,[21−23] and stacking along the DNA template.[23−31] The basic observation is that *meso*-tetrakis(*N*-methylpyridinium-4-yl)porphyrin (herein referred to as TMPyP, Figure 1), a representative of the DNA binding cationic porphyrin family, intercalates between CpG sequences.[1,2,32,33] The amine moiety at the G base that protrudes into the minor groove has been shown to play an essential role in TMPyP intercalation.[12] TMPyP also intercalates into native DNA containing GC base pairs at low [porphyrin]/[DNA] ratios (herein referred to as the *R* ratio).[34,35] The external binding modes which take place at the AT polynucleotides or native DNA at high *R* ratios may be classified into three categories namely monomeric groove binding and moderate and extensive stacking. These external binding modes have been shown to be clearly distinguishable by circular dichroism (CD) spectroscopy. At low *R* ratios, TMPyP binds at the minor groove of the AT-rich polynucleotides producing a positive CD signal in the Soret absorption region.[29,36,37] TMPyP has been shown to bind

Received: August 14, 2012
Revised: September 19, 2012
Published: September 22, 2012

   dx.doi.org/10.1021/jp3081063 | *J. Phys. Chem. B* 2012, 116, 12510−12521

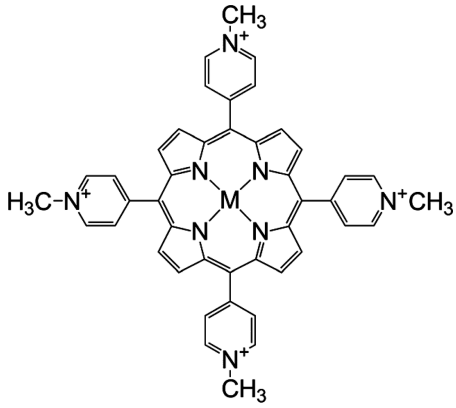

Figure 1. Chemical structure of metallo *meso*-tetrakis(*N*-methylpyridinium-4-yl)porphyrin. M = Ni(II), Cu(II), V(IV)=O, Ti(IV)=O, Co(III), and Mn(III).

across the minor groove in this case. As the *R* ratio increases, the majority of TMPyP either moderately or extensively stacks outside of the DNA stem. This extensive stacking of TMPyP is related to the inducement of DNA aggregation. These two types of stacking can be distinguished by their characteristic bisignate CD spectra.[19,30] Moderate stacking was shown to occur in the major groove of AT-rich oligonucleotides.[29]

The nature of the central metal ion is one of the important factors that determine the binding mode.[1,38−55] In general, introducing metal ions which lack an axial ligand, such as Cu(II), Ni(II), or Au(III), into TMPyP does not affect its binding mode. These planar porphyrins also intercalate at the GC polynucleotides or GC site of native DNA at low *R* ratios. However, TMPyP with a central metal ion that possesses one or two axial ligands, such as Zn(II), Co(III), Fe(III), Mn(III), V(IV)=O, or Ti(IV)=O, appear to be incapable of intercalation. They exhibit the external binding mode. The incline angles of the porphyrin ring system of ZnTMPyP with respect to the local DNA helix axis obtained from a linear dichroism (referred to as LD) study were 62°−67°,[39] whereas that of CoTMPyP was 58 ± 1°.[45] VOTMPyP was reported to be the hexa-coordinated $OV^{IV}(H_2O)(TMPyP)^{4+}$ form in aqueous solution. The hexa-coordinated form remained when bound to poly[d(A-T)$_2$], whereas the sixth coordinated H_2O was removed in the complex formed with poly[d(G-C)$_2$].[43] All of these observations indicated that metallo-TMPyP (herein denoted by MTMPyP) with one or two axial ligands at the central metal ion does not intercalate between DNA base-pairs, but produces an external binding mode. In spite of the abundance of work on the interaction of MTMPyP and DNA, all of the results were obtained using different conditions and methods. Therefore, in this study, we systematically investigated the binding geometry and binding mode of MTMPyPs under the same condition using polarized spectroscopy, namely CD and LD. A similar study has appeared at low *R* ratios ($R < 0.025$). Under this condition, the binding modes were independent of the *R* ratio, suggesting that the interaction between DNA-bound porphyrins were negligible.[56] TMPyP and the MTMPyP with central metal ions lacking axial ligands intercalated between DNA base pairs, whereas those with an axial ligand, namely VOTMPyP, TiOTMPyP, and CoTMPyP, were suggested to bind at the minor groove. The angle of B_x and B_y transition moments with respect to the local DNA helix axis of latter porphyrins were 39°∼46° at the *R* ratio under 0.025. Following the previous study, the *R* ratios adopted in this study were in the range from 0.02 to 0.16, representing monomeric binding to moderately stacked binding mode. The central metals investigated in this study were Cu and Ni, representing the planar TMPyP, VO, and TiO as representatives of *penta*-coordinated TMPyP and Co and Mn as *hexa*-coordinated TMPyP.

EXPERIMENTAL SECTION

Materials. TMPyP, NiTMPyP, and TiOTMPyP were purchased from Frontier Scientific, Inc. (Utah, U.S.A.). CoTMPyP and CuTMPyP were obtained from Midcentury (Chicago, IL), and VOTMPyP was from Porphyrin Products (Logan, Utah). All porphyrins purchased were in the chloride salt form. The purities of porphyrins were checked by the appearance of single spot on TLC under the reported condition[57] and were used without further purification. Calf thymus DNA, purchased from Worthington (Lakewood, NJ), was dissolved in 5 mM cacodylate buffer, pH 7.0, by exhaustive shaking at 4 °C. This buffer solution was used throughout this study. The concentrations of the porphyrins were determined using their molar extinction coefficients:[58,59] ε_{421nm} = 245 000 M^{-1} cm^{-1} for TMPyP, ε_{418nm} = 150 000 M^{-1} cm^{-1} for NiTMPyP, ε_{424nm} = 231 000 M^{-1} cm^{-1} for CuTMPyP, ε_{438nm} = 207 000 M^{-1} cm^{-1} for VOTMPyP, ε_{436nm} = 150 000 M^{-1} cm^{-1} for TiOTMPyP, and ε_{434nm} = 215 000 M^{-1} cm^{-1} for CoTMPyP. In the MnTMPyP case, two coefficients namely ε_{463nm} = 93 000 and 130 000 M^{-1} cm^{-1} have been reported,[47,60] and the latter value was confirmed correct. The molar extinction coefficient for DNA is ε_{260nm} = 6700 M^{-1} cm^{-1}. All of the measurements were performed at ambient temperature (∼20 °C). The appearance of spectra for the porphyrin−DNA system may be affected by the order of mixing.[61] Therefore, samples were prepared by adding aliquots of concentrated porphyrin solution to appropriate DNA solution (typically up to 100 μL to 3 mL) before measurements, and the signals were corrected for volume changes.

Absorption and CD. The intercalation of planar aromatic molecules between DNA base-pairs manifests itself by a large red-shift and hypochromism in the absorption band due to the π−π interaction between the nucleobases and the intercalating molecules. In the case of molecules binding to the minor groove, a large alteration in the absorption band is related to the change in the molecular conformation of the binding molecule. The absorption spectra of TMPyP and MTMPyP in the presence and absence of DNA were recorded on a Cary 100 spectrophotometer (Palo Alto, CA). The interaction of the chirally arranged electric transition moment of the nucleobases with that of the porphyrins induces a characteristic CD spectrum, particularly in the Soret band, although the porphyrin itself is an achiral molecule. The appearance of CD spectrum may be considered to be a diagnostic for the porphyrin binding mode. Although an exception has been reported,[52] a negative CD signal in the Soret band represents intercalation, whereas a positive CD signal is related to monomeric groove binding. A bisignate CD spectrum in the Soret band has been considered to be indicative of porphyrin stacking along the DNA stem. The CD spectra were recorded using either a Jasco J-715 or J-810 spectroporlarimeter (Tokyo, Japan). The CD spectra were averaged over an appropriated number of scans when necessary.

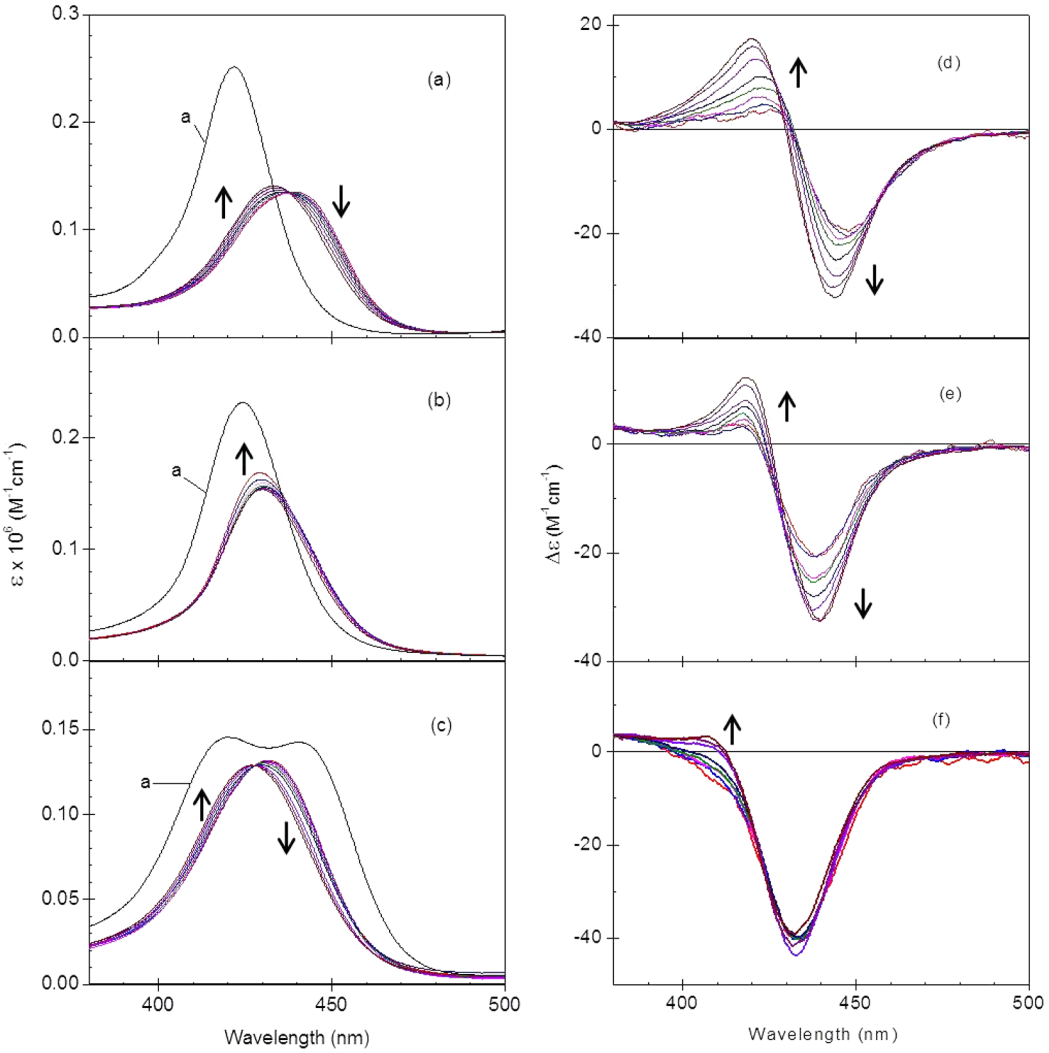

Figure 2. Absorption and CD spectra of TMPyP (panels a and d, respectively), CuTMPyP (panels b and e, respectively), and NiTMPyP (panels c and f, respectively) associated with DNA in the Soret region. The black curve, denoted by a, represents the absorption spectra of the corresponding porphyrins in the absence of DNA. [DNA] = 100 μM. R = 0.02, 0.04, 0.06, 0.08, 0.10, 0.12, 0.14, and 0.16. The R ratio increases in the direction of the arrows.

LD. LD has been proven to be a powerful technique and is defined as[62,63]

$$\mathrm{LD}(\lambda) = A_{\parallel}(\lambda) - A_{\perp}(\lambda) \quad (1)$$

where $A_{\parallel}(\lambda)$ and $A_{\perp}(\lambda)$ are the absorption spectra measured with the light plane polarized parallel and perpendicular, respectively, to the oriented sample, DNA in the current study. The orientation of the DNA sample was achieved by flow using a Couette cell of the Wada type.[64] Measured LD is divided by isotropic absorption spectrum, resulting in a dimensionless quantity called the reduced linear dichroism (referred to as LD^r), which is related to the orientation factor (S), the ability of the sample to orient, and the optical factor (O) through

$$\mathrm{LD}^r(\lambda) = S \times O = 1.5S(\langle 3\cos^2\alpha\rangle - 1) \quad (2)$$

The orientation factor describes the degree of orientation of the DNA helix in the gradient shear, depending on various factors, including the stiffness and contour length of the DNA, the flow rate, the viscosity of the medium, and the temperatures. All of these factors can be kept fixed by keeping the experimental conditions constant, except for the contour length of the DNA which is affected by the binding of the molecules to DNA. The optical factor is related to the angle, α, which is the angle of the electric transition moment of the DNA-bound molecules with respect to the local DNA helix axis. The bracket denotes the average angle. The S value can be determined by assuming an average angle of 86° between the DNA base plane and the local DNA helix axis, and consequently, the angle α can be determined. A constant, wavelength-independent LD^r in the molecule's absorption region is expected when the DNA-bound molecule possesses one electric transition moment and the binding mode is homogeneous. However, if the binding mode is heterogeneous or two or more transition moments are involved, the LD^r would be wavelength-dependent.

RESULTS

In the system adopted in this study, the presence of free-porphyrins may affect the result, especially LD, because the LD reflects only the DNA-bound porphyrin: DNA unbound porphyrin cannot be oriented in the flow, resulting in a reduced LD magnitude. The equilibrium constants of TMPyP and CuTMPyP were reported as 1.0×10^7 and 1.2×10^7 M^{-1}, respectively, at the ionic strength of 0.2 M.[42] Applying these

dx.doi.org/10.1021/jp3081063 | J. Phys. Chem. B 2012, 116, 12510−12521

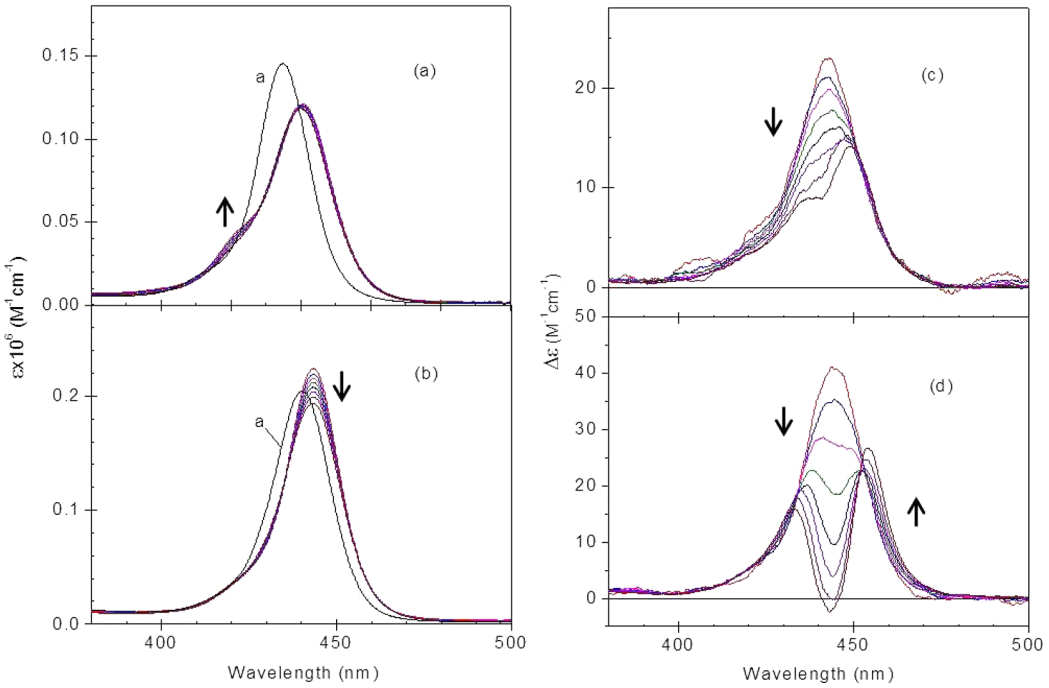

Figure 3. Absorption and CD spectra of TiOTMPyP (panels a and c, respectively) and VOTMPyP (panels b and d, respectively) complexed with DNA in the Soret region. The black curve, denoted by a, represents the absorption spectra of the corresponding porphyrins in the absence of DNA. [DNA] = 100 μM. R = 0.02, 0.04, 0.06, 0.08, 0.10, 0.12, 0.14, and 0.16. The R ratio increases in the direction of the arrows.

equilibrium constants, DNA-unbound TMPyP was below 0.6%. Furthermore, it has been well-known that decreasing in ionic strength as well as increasing in the number of positive charges on the porphyrin molecules increases the porphyrin's equilibrium constant.[42] The ionic strength in this study was 5 mM, and the number of positive charges in the MTMPyP is higher compared to TMPyP. All of these factors ensure that the amount of DNA-unbound porphyrin is negligible.

Absorption and CD Spectra of Planar Porphyrins. The absorption and CD spectra of the planar porphyrins, namely TMPyP, CuTMPyP, and NiTMPyP, bound to DNA are depicted in Figure 2. At the lowest R ratio (R = 0.02), TMPyP exhibited hypochromism of about 45% and a red-shift of 16 nm upon binding to DNA. The maximum in the absorption spectrum for the DNA-bound TMPyP was found at 439 nm (panel a). Increasing the R ratio resulted in a decrease in the absorbance at long wavelengths and an increase at short wavelengths. At R = 0.16, the maximum was found at 433 nm. An isosbestic wavelength at 436 nm was also apparent, suggesting that these changes in the absorption spectrum occurred between two bound species. A negative CD band in the Soret region centered at 448 nm was apparent for the TMPyP−DNA complex at R = 0.02, which is a diagnostic for the intercalation binding mode (panel d). Upon increasing the R ratio, a positive band was built up at short wavelengths, whereas the negative band shifted to 444 nm and its magnitude increased. At R = 0.16, the CD spectrum of the TMPyP−DNA complex appeared to be bisignate with its positive maximum at 420 nm and its negative minimum at 444 nm, suggesting the occurrence of an intermolecular interaction between the electric transition moments of the DNA-bound TMPyPs. CuTMPyP exhibited ∼30% hypochromism and a red-shift of 6 nm (from 423 to 429 nm) in the absorption spectrum upon binding to DNA. Increasing the R ratio resulted in an increase in absorbance with a slight shift of the maximum to shorter wavelengths (panel b). The pattern of change in the CD spectrum of the DNA-bound CuTMPyP (panel d) was similar to that observed from TMPyP: the negative band at 438 nm at the lowest R ratio (R = 0.02) changed to bisignate CD with its positive maximum at 418 nm and negative minimum at 439 nm at the highest R ratio (R = 0.16). In the case of NiTMPyP (panel c), maxima at 418 and 442 nm were apparent in the absence of DNA. The binding of NiTMPyP to DNA resulted in an absorption maximum at 431 nm and a decrease in absorbance by ∼10%. Similarly to TMPyP, an increase in the R ratio resulted in a decrease in the absorbance in short wavelength region and increase in long wavelength region. This change was accompanied by an isosbestic point at 428 nm. As shown in Figure 2 (panel f), NiTMPyP also produced a negative CD band centered at 432 nm at a low R ratio upon complexation with DNA. Increasing the R ratio resulted in the appearance of the positive band in the short wavelength region, although it was significantly less effective compared to CuTMPyP and TMPyP.

Absorption and CD Spectra of Porphyrins with Axial Ligands. Figure 3 depicts the absorption and CD spectra of VOTMPyP and TiOTMPyP in the presence of DNA. As observed for the planar porphyrins, TiOTMPyP produced hypochromism and a red-shift of 6 nm from 434 nm in the absorption maximum when it associated with DNA (Figure 3, panel a). The effect of increasing the R ratio on the absorption spectrum was negligible in the case of TiOTMPyP, except for a very small increase near the shoulder at about 420 nm. A positive CD in the Soret band centered at 443 nm was observed for TiOTMPyP in the presence of DNA at an R ratio of 0.02 (panel c), which is in contrast to the negative CD in the case of planar porphyrins. As the R ratio increased, the magnitude of the CD spectrum seemed to decrease. At the highest mixing ratio (R = 0.16), a negative band in the CD spectrum centered at 441 nm was observed. A considerable change in the CD

dx.doi.org/10.1021/jp3081063 | J. Phys. Chem. B 2012, 116, 12510−12521

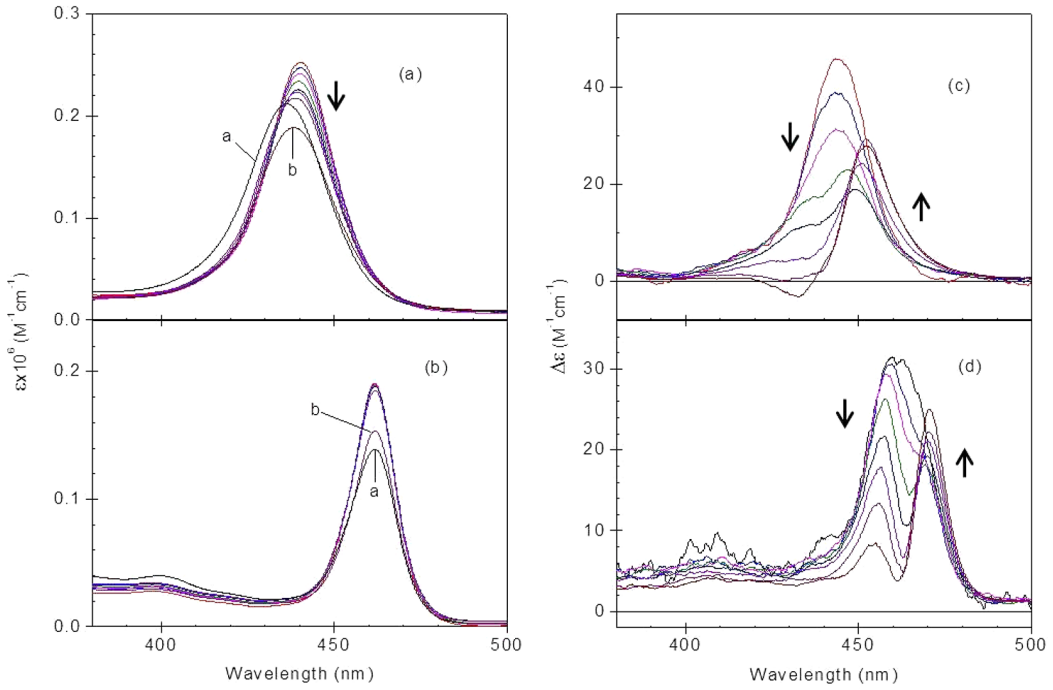

Figure 4. Absorption and CD spectra of CoTMPyP (panels a and c, respectively) and MnTMPyP (panels b and d, respectively) complexed with DNA in the Soret region. The black curve, denoted by a, represents the absorption spectra of the corresponding porphyrins in the absence of DNA. [DNA] = 100 μM. R = 0.02, 0.04, 0.06, 0.08, 0.10, 0.12, 0.14, and 0.16. The R ratio increases in the direction of the arrows. In panels a and c, the absorption spectrum of the CoTMPyP−DNA and MnTMPyP−DNA complexes at R = 0.16 is denoted by b.

spectrum was noticed to start even at a very low R ratio, in spite of the conserved absorption spectrum, suggesting that the interaction between the electric transition moments of the DNA-bound porphyrins started at a very low R ratio. VOTMPyP exhibited different behavior in its absorption spectrum. It produced hyperchromism upon binding to DNA at low R ratios: the absorbance increased by 15% (Figure 3, panel b), which was in contrast to the planar porphyrins. The maximum shifted to a longer wavelength compared to DNA-free VOTMPyP (from 438 to 443 nm). Upon increasing the R ratio, the absorbance started to decrease without any shift in its maximum. The binding of VOTMPyP to DNA induced a positive CD spectrum centered at 445 nm at the lowest R ratio. The change in the CD spectrum with increasing R ratio was significant: a negative band ca. 445 nm was noticed at an R ratio as low as 0.08, which became more negative as the R ratio increased.

Similarly to VOTMPyP, hyperchromisms in their absorption spectra were observed for CoTMPyP and MnTMPyP at R = 0.02, as shown in Figure 4 (panels a and d), respectively. In the case of CoTMPyP, the absorbance increased by ∼16% and the maximum shifted to a longer wavelength by 4 nm (from 436 to 440 nm). The increase in the R ratio resulted in a gradual decrease in the absorbance with the maximum shifted to a shorter wavelength. On the other hand, the degree of hyperchromism for MnTMPyP was ∼40% and the absorption maximum remained at the same wavelength (462 nm). The decrease in the absorbance at the maximum with increasing R ratio was very small in the case of MnTMPyP. It is noticed that when the R ratio was above 0.14 both the CoTMPyP−DNA and MnTMPyP−DNA complexes tended to aggregate. The aggregation, which formed immediately after mixing the porphyrins, can be noticed by the naked eye. Formation of aggregation was previously reported for the MnTMPyP−DNA mixture at high R ratio and high ionic strength.[65] On the other hand, no aggregations were observed from both CoTMPyP−DNA and MnTMPyP−DNA complexes at the R ratio below 0.14 for at least 3 d after mixing. The large deviation in the absorption spectrum at R = 0.16 (curve denoted by b in panel a and b, Figure 4) for the CoTMPyP−DNA and MnTMPyP−DNA complex may be ascribed to its aggregation. Similarly to VOTMPyP and TiOTMPyP, both CoTMPyP and MnTMPyP produced a positive CD signal in the Soret band with maxima at 444 and 459 nm, respectively (Figure 4, panels c and d, respectively). In the case of CoTMPyP, a significant decrease in the CD magnitude in the short wavelength region was apparent, which was accompanied by an increase in the long wavelength region. A decrease in the CD spectrum, i.e., the formation of a minimum at 463 nm was noticed for MnTMPyP with a slight increase in the CD magnitude at long wavelengths. This observation suggested that the interaction of the electric transition moments of the bound CoTMPyP as well as MnTMPyP started at a very low R ratio.

LD and LD^r Spectra. The LD spectra of the planar porphyrin−DNA complexes, TMPyP, CuTMPyP, and NiTMPyP, are shown in Figure 5, panels a−c, respectively. The appearances of the LD for all three complexes were almost identical and were characterized by a large negative signal in both the DNA absorption region and in the Soret region. A negative LD in the DNA absorption region was expected from the setup adopted in this work.[62−64] As the R ratio increased, positive contributions at 268−270 nm were apparent for all three porphyrins. This positive contribution may arise either from the tilt of the DNA bases or from the tilted electric transition of porphyrin or from both. At this stage, none of these contributions can be clearly separated and, thus, will not be discussed any further. In the Soret region, the negative maximum was found at 444 nm for TMPyP and 436 nm for

dx.doi.org/10.1021/jp3081063 | J. Phys. Chem. B 2012, 116, 12510−12521

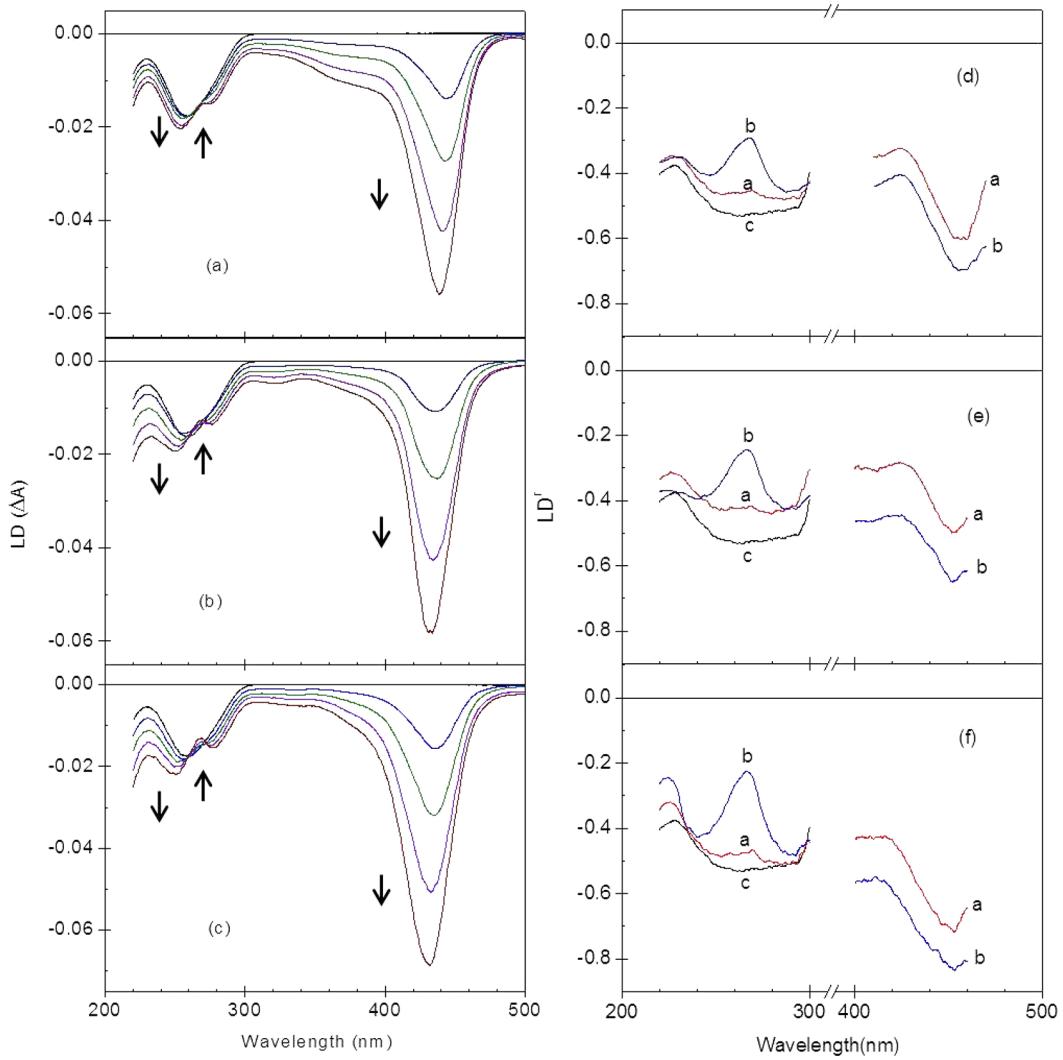

Figure 5. LD and LD^r spectra of TMPyP (panels a and d, respectively), CuTMPyP (panels b and e, respectively), and NiTMPyP (panels c and f, respectively) associated with DNA. [DNA] = 100 μM. Although the LD spectra were recorded at R = 0.02, 0.04, 0.06, 0.08, 0.10, 0.12, 0.14, and 0.16, only those of R = 0.04, 0.08, 0.12, and 0.16 are shown to avoid complication. The R ratio increases in the direction of the arrows. In the case of LD^r, the porphyrin-free DNA (denoted by c) and those with the lowest (R = 0.02, curve a) and highest (R = 0.16, curve b) mixing ratios are shown.

both CuTMPyP and NiTMPyP. The LD maximum shifted by ~5 nm to shorter wavelengths at R = 0.16 for all three complexes. The large negative LD in the Soret absorption region suggests that the B_x and B_y transitions of the porphyrins tilt to a large extent with respect to the local DNA helix axis. The measured LD was divided by the absorption spectrum to obtain the LD^r spectra, which are depicted in Figure 5, panels d–f, for the TMPyP–DNA, CuTMPyP–DNA, and NiTMPyP–DNA complexes, respectively. In addition to the LD, the shape of the LD^r spectra appeared to be similar for all three complexes. At a low R ratio, the LD^r spectra were characterized by a decreased magnitude in the DNA absorption region and were largely wavelength-dependent in the Soret region. The latter observation suggests that the two electric transition moments were skewed in the intercalation pocket. The magnitudes in the Soret region were similar to or larger than those in the DNA absorption region. The larger LD^r magnitude at the maximum in the Soret region compared to that in the DNA absorption region prevented the calculation of the angle, α, in eq 2, because an imaginary number was involved in the calculation. However, a larger or comparable LD^r magnitude in the molecule's absorption region has frequently been observed for intercalating molecules.

DNA-bound TMPyPs with an axial ligand also produced a negative LD in the Soret absorption region at low R ratios. Figure 6 depicts the LD spectra of TiOTMPyP (panel a) and VOTMPyP (panel b) and those of CoTMPyP (panel a) and MnTMPyP (panel b) are displayed in Figure 7. The negative maxima at 442, 439, 449, and 460 nm were apparent for TiOTMPyP, VOTMPyP, CoTMPyP, and MnTMPyP, respectively. In the case of TiOTMPyP, a shoulder at ca. ~423 nm was also apparent. However, the magnitudes of the LD in the Soret region for all of the porphyrins with axial ligands were significantly smaller than those of the planar porphyrins. Increasing the R ratio resulted in the production of a bisignate LD spectrum in this region for VOTMPyP and MnTMPyP. At R = 0.16, the highest R ratio adopted in this study, the LD exhibited bisignate signals: negative minimum at 439 nm and positive maximum at 453 nm for the VOTMPyP–DNA complex (Figure 6, panel c). The negative minimum at 460 nm and a maximum at 469 nm were observed for the MnTMPyP–DNA complex at R = 0.14 (Figure 7, panel b).

dx.doi.org/10.1021/jp3081063 | J. Phys. Chem. B 2012, 116, 12510–12521

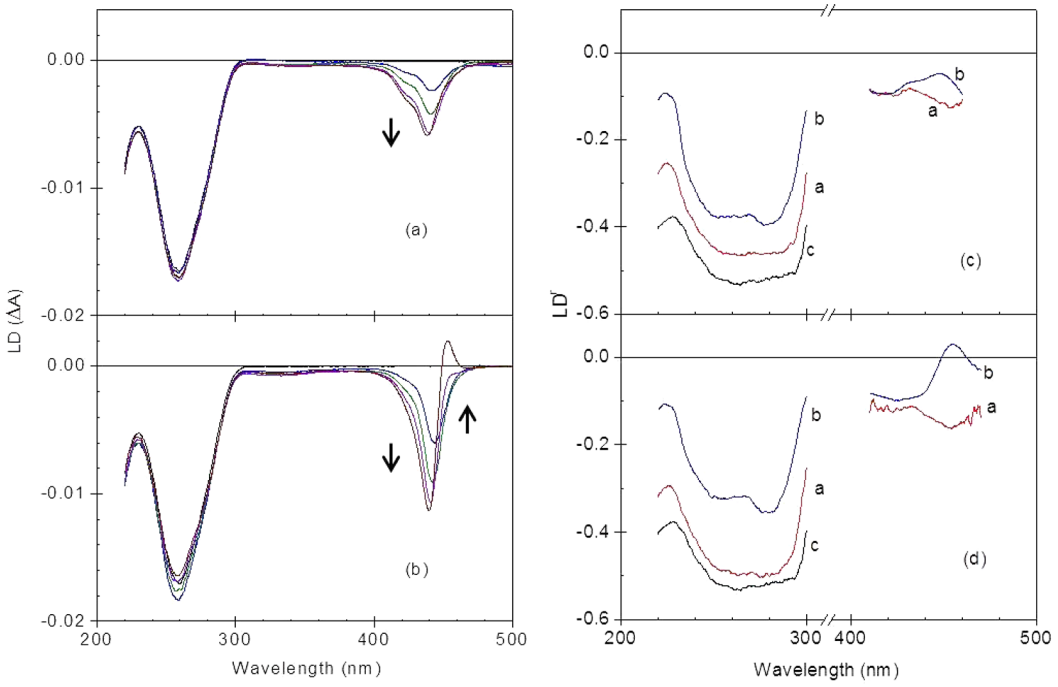

Figure 6. LD and LD^r spectra of TiOTMPyP (panels a and c, respectively) and VOTMPyP (panels b and d, respectively) associated with DNA. The other conditions are the same as those in Figure 5.

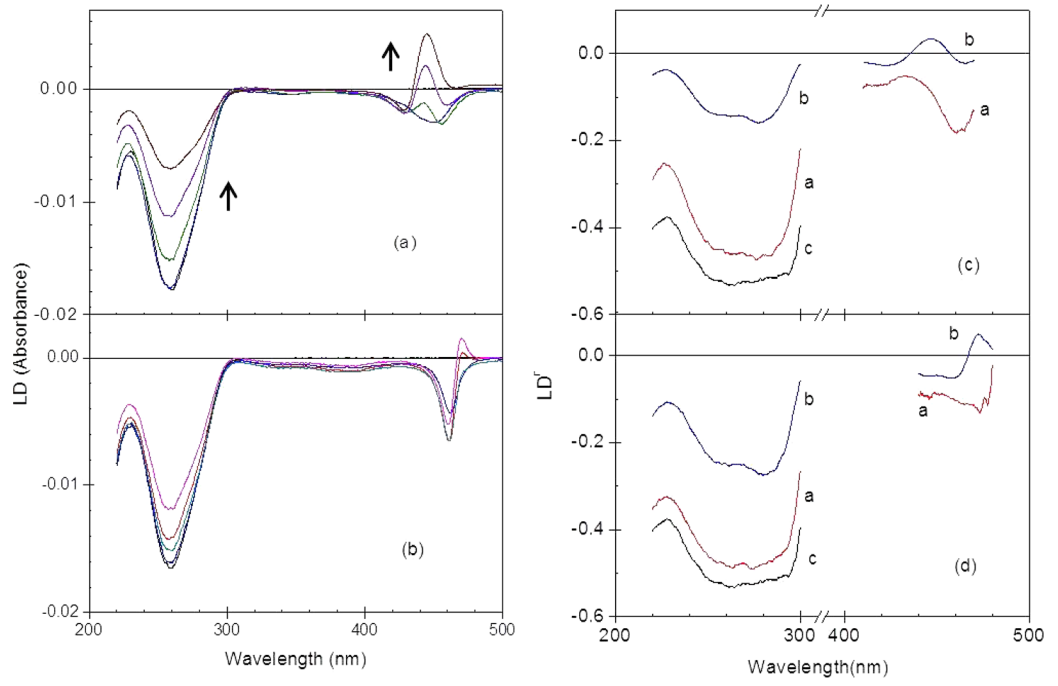

Figure 7. LD and LD^r spectra of CoTMPyP (panels a and c, respectively) and MnTMPyP (panels b and d, respectively). Although the other conditions are the same as those in Figure 5, both LD and LD^r at R = 0.16 were replaced by R = 0.14, because both the MnTMPyP−DNA and CoTMPyP−DNA complex at R = 0.16 started to aggregate (see text).

The LD spectrum produced by the CoTMPyP−DNA complex was even more complicated. It produced negative minima at 429 and 458 nm and a positive maximum at 444 nm at R = 0.14 and, again, at R = 0.16, the CoTMPyP−DNA and MnTMPyP−DNA complexes started to aggregate. TiOTMPyP exhibited contrasting LD behavior. As the R ratio increased, the magnitude gradually increased while retaining its overall shape. At the highest R ratio (0.16), the negative maximum shifted to 439 nm. The magnitude of the LD remained above at R = 0.12. Figures 6 panel c and d show the LD^r spectra of TiOTMPyP and VOTMPyP complexed with DNA at two extreme R ratios (R = 0.04 and 0.16). Those for CoTMPyP and MnTMPyP at R = 0.04 and 0.14 are depicted in Figure 7, panels c and d, respectively. The LD^r spectra in the Soret region varied with the wavelength for all of the TMPyPs with axial ligands, and the magnitude in this region was significantly

dx.doi.org/10.1021/jp3081063 | J. Phys. Chem. B 2012, 116, 12510−12521

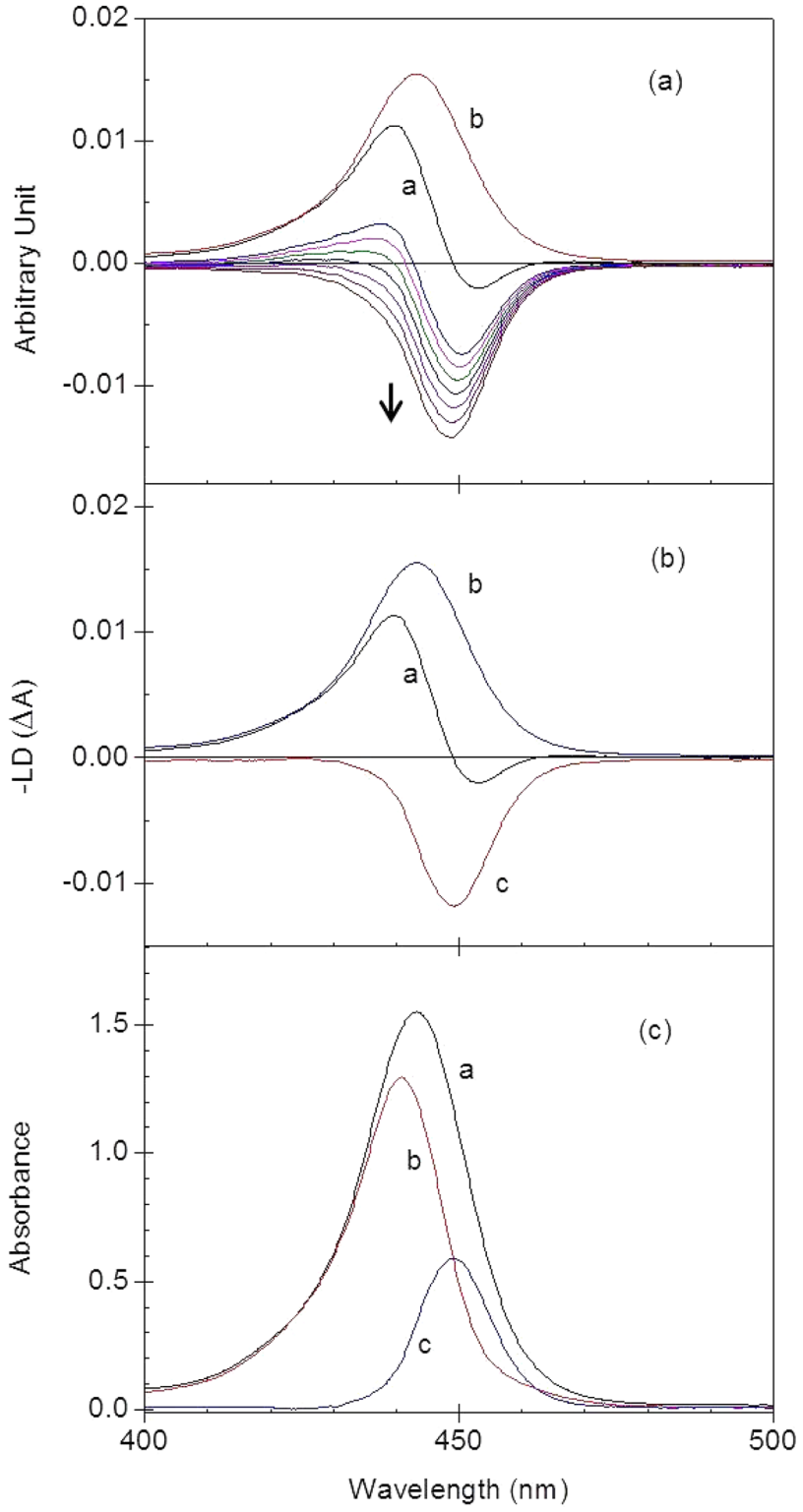

Figure 8. (a) Difference spectra, $LD_2(\lambda) = LD - \kappa A(\lambda)$, of VOTMPyP bound to DNA. [DNA] = 100 μM. R = 0.16. Curves a and b denote the measured LD spectrum multiplied by −1 and the absorption spectrum divided by 100, respectively. The continuous curves representing $LD_2(\lambda)$ were obtained from the κ value of ∼0.006−0.012 with an increment of 0.001. The LD with κ = 0.01 (marked by red) was considered the most representative profile of the long-wavelength transition, $LD_2(\lambda)$. (b) The measured LD spectrum (curve a) of the VOTMPyP−DNA complex was resolved into the contributions of the two transitions (curves b and c). (c) The measured absorption spectrum (curve a) and contribution from the two absorption spectra corresponding to the B_x and B_y transitions (curves b and c) obtained in similar manner to the analysis of the LD spectrum.

smaller than that in the DNA absorption region. This observation was in contrast with the planar porphyrins. The positive contribution in the DNA absorption region that was observed for the planar porphyrins at a high R ratio was far less significant. Upon increasing the R ratio, the magnitude of LD^r in the DNA absorption region decreased. All of these results

dx.doi.org/10.1021/jp3081063 | J. Phys. Chem. B 2012, 116, 12510−12521

suggested that the average angle of the molecular plane of the TMPyP was greatly tilted with respect to the local DNA helix axis.

Analysis of LD Spectra of the Porphyrins with Axial Ligand Bound to DNA. The strong wavelength dependence of the LD^r magnitude in the Soret region of the porphyrins with an axial ligand implied that the degeneracy of the two transition moments (B_x and B_y transitions) of the porphyrin was partially removed upon binding to DNA by having different angles with respect to the local DNA helix axis. If this is the case, the LD^r may be analyzed by noticing that the absorption and LD spectra are the sum of the contributions from two transitions by employing a similar approach to that used for the TMPyP complexed with poly[d(I−C)$_2$],[12] and poly[d(A-T)$_2$] and poly(dA)·poly(dT).[36] For the LD spectra,

$$\mathrm{LD}(\lambda) = a_1\mathrm{LD}_1(\lambda) + a_2\mathrm{LD}_2(\lambda) \quad (3)$$

where $\mathrm{LD}_1(\lambda)$ and $\mathrm{LD}_2(\lambda)$ are the LD profiles of the B_x and B_y transitions, respectively, contributing to the LD spectrum. a_1 and a_2 are coefficients. The contribution of one of the LD spectra say, $\mathrm{LD}_2(\lambda)$, can be obtained by the subtraction of the properly tuned absorption spectrum, because the contributions of the two transitions to the absorption and LD spectra are different (eq 4).

$$\mathrm{LD}_2(\lambda) = \mathrm{LD} - \kappa A(\lambda) \quad (4)$$

where κ is a weighting factor and $A(\lambda)$ is the measured absorption spectrum. Figure 8 panel a shows the measured LD spectrum and absorption spectrum divided by 100 for the VOTMPyP-DNA complex as an example. The $\mathrm{LD}_2(\lambda)$ spectrum with a κ value of 0.006−0.012 with increment of 0.001, of which the LD spectrum obtained from κ = 0.01 was considered to represent the LD spectrum of the long-wavelength transition, is also shown in Figure 8, panel a. The resulting LD spectra consisted of a positive band with its maximum at 442 nm and a negative band with its minimum at 449 nm (Figure 8, panel b). Similarly, the measured absorption spectrum was resolved into the contributions of the two absorption spectra representing the B_x and B_y transitions (Figure 8, panel c). The maxima of the two resulting absorption spectra were at 441 and 449 nm, respectively. Once the absorption and LD spectra are resolved, the calculation of the LD^r values for the B_x and B_y transitions is simple. Consequently, the S value was obtained from eq 2 by assuming that the LD^r value at 260 nm represents the average angle of the DNA base plane with respect to the local DNA helix axis, which allowed the calculation of the angle, α, of the electric transition moments. Similar calculations were repeated for TiOTMPyP, CoTMPyP, and MnTMPyP complexed with DNA at two extreme R ratios and the resulting angles are summarized in Table 1. At R = 0.04, one of the transition moments, say the B_y transition, of VOTMPyP, CoTMPyP, and MnTMPyP bound to DNA lies at an angle of 63°∼65° relative to the DNA helix axis, and the other (B_x transition) is tilted by an angle of 6°∼8° from the first one to an angle of 57°∼59°. The TiOTMPyP−DNA complex exhibited somewhat lower tilt angles of ∼56° and ∼59° for the B_x and B_y transitions, respectively. At a high R ratio, the binding geometries of VOTMPyP and MnTMPyP were almost identical: the angle between the B_y transition and the DNA helix axis remained the same as that at the low R ratio, whereas that corresponding to the B_x transition moment was small, viz. 42°∼43°. The extent of this type of change in the binding angles was less for the TiOTMPyP−DNA complex: the angles were 52° and 60°, respectively. In the case of the CoTMPyP−DNA complex, the angles were impossible to be resolved by the above-described method at the high R ratios. The stepwise reduction of the absorption spectrum from the LD did not result in a one simple peak, as might be expected from the complicated LD^r spectrum (Figure 7, panel c) with multiple minima. As previously mentioned, CoTMPyP may have multiple binding modes to DNA, including its aggregation, in the R ratio range adopted in this study.

Table 1. Resolved Angles of Electric Transition Moments in the Soret Band of the DNA-Bound MTMPyP Possessing Axial Ligand(s) with Respect to the Local DNA Helix Axis

	R = 0.04	R = 0.16
TiOTMPyP	56°, 59°	52°, 60°
VOTMPyP	59°, 63°	43°, 63°
CoTMPyP	57°, 64°	n.a.[a]
MnTMPyP	57°, 65°	41°, 64°

[a]Not available: the LD^r spectrum for the CoTMPyP−DNA complex at R = 0.14 was so complicated that it could not be resolved by the method described in the text. The CoTMPyP−DNA complex with an R ratio above 0.16 started to aggregate.

DISCUSSION

Stacking of Planar Porphyrins. The absorption and polarized spectroscopic characteristics of planar porphyrin, particularly TMPyP, complexed with double stranded native DNA and synthetic polynucleotides have been well documented. Upon binding to poly[d(G-C)$_2$] or native DNA, TMPyP was reported to produce a negative CD band and large red-shift and hypochromism in the absorption spectrum in the Soret absorption region, which has been considered as a diagnostic for the intercalative binding mode.[12,18,66] In contrast, TMPyP associated with poly[d(A-T)$_2$] or poly(dA)·poly(dT) produces a positive CD signal, reflecting a minor groove binding mode.[29,30,36] The CD spectrum changes toward the bisignate form as the R ratio increases when TMPyP is complexed with either DNA or an AT-rich polynucleotide. Thus, the negative CD signal and changes in the absorption spectrum compared to that in the absence of DNA that were observed in this study for TMPyP, CuTMPyP, and NiTMPyP should be considered as the reflection of the intercalative binding mode. However, the configuration of the porphyrins in the intercalation pocket deviates from those of classical intercalators: the molecular plane of the porphyrin is not planar. The angle of either the B_x or B_y electric transition of the porphyrin or both tilt to a large extent with respect to the local DNA helix axis (flow direction), as evidenced by the large wavelength-dependent LD^r spectrum in the Soret region. Furthermore, the DNA base planes also tilt from the flow direction.

The appearance of bisignate CD, which is particularly noticeable for TMPyP and CuTMPyP and in less extent for NiTMPyP, with increasing R ratio is accompanied by an enhancement in intermolecular porphyrin interactions. The shape of intercalated porphyrins is invariant of the mixing ratio at low [porphyrin]/[DNA] ratios,[56] and the exciton coupling between intercalated porphyrin does not likely occur. One of the possible reasons for observed resonance is that the second porphyrin binds to the outside of the DNA at the vicinity of the first one which is intercalated. Indeed, there have been several

reports supporting the presence of outside binding mode. For example, although NiTMPyP intercalated to poly[d(G-C)$_2$],[1] it exhibited an outside binding mode when bound to AT-rich polynucleotides.[41,67−69] However, the appearance of the LD^r signal in the Soret region seems to be conserved at high R ratios, suggesting that the binding geometry was conserved in the R ratio range adopted in this study. The only possibility to produce the conserved LD^r is that the binding geometry of the second porphyrin, located near the first one, probably outside of DNA, is the same as that of the first one. The other explanation for the appearance of a bisignate CD signal with conserved LD^r is the interaction of the porphyrins between intercalated ones, i.e., coupling of the electric transition moments of the nearby intercalated porphyrins. Considering the nearest neighboring site exclusion model for the intercalation of any molecule between a DNA base pair, the intercalation of the second porphyrin occurs at the intercalation site situated at a distance of two base-pairs at the nearest. Thus, the coupling between the electric transition moments of the two intercalated planar porphyrins conceivably occurs even when two or more DNA base pairs are present between them. The two transitions, B_x and B_y of the interacting porphyrins are parallel each other. At this stage, available evidences are insufficient to support or reject either of the possibilities.

Behavior of Porphyrins with Axial Ligand. The absorption, CD, and LD^r spectral properties of VOTMPyP and MnTMPyP associated with DNA can similarly summarized as hyperchromism and a relatively small red-shift in their absorption spectrum, a positive CD, and largely distorted LD^r in the Soret region at the lowest R ratio (0.02−0.04). The angles of the two electric transitions were 57°∼59° and 63°∼65° relative to the DNA helix axis. In the case of MnTMPyP, the incline angle of the porphyrin ring system with respect to the local DNA helix axis is slightly smaller than that obtained from the unresolved LD^r value in the Soret region.[39] These spectral properties indicate that the binding modes of VOTMPyP and MnTMPyP are similar and that they bind outside of DNA in accordance with the reported results.[39,52,54] Particularly, the measured angles of the electric transition moments cannot be the result of intercalation. Increasing in the porphyrin population relative to the DNA resulted in similar spectral changes for both VOTMPyP and MnTMPyP: a slight decrease in absorbance and the appearance of a minimum in the CD spectrum. These spectral changes were accompanied by a decrease in the tilt angle of one of the electric transition moments relative to the DNA helix axis. As the R ratio increased, the angle of one of the electric transition moments decreased from 57°∼59° to 42°∼43°, whereas the other remained. These observations suggest that the externally bound porphyrins also interact with each other when the relative population increased, i.e., coupling occurs between the electric transitions moments of the porphyrins. The nature of this interaction may be different from that of the intercalated porphyrins. In contrast with the planar porphyrins, whose electric coupling occurs between parallel intercalated porphyrins, those with axial ligands cannot be parallel due to their axial ligands.

The behavior of CoTMPyP when bound to DNA was similar to that of VOTMPyP and MnTMPyP at low R ratios. The spectral properties are summarized as hyperchromism and a small red-shift in the absorption spectrum, a positive CD band, and the negative, wavelength-dependent LD^r spectrum in the Soret region. From the LD^r spectrum, the angles of the two electric transition moments were found to be 57° and 64°, which is the same as those observed for VOTMPyP and MnTMPyP. All of these spectral properties suggest that the binding mode of CoTMPyP to DNA at low R ratios is similar to those of the two previously discussed metalloporphyrins. Increasing in the porphyrin density resulted in a decrease in the absorbance and CD intensity. Although the decrease in absorbance was similar to that observed in the case of VOTMPyP, the pattern of change in the CD spectrum was different: a decrease in the short wavelength region was apparent instead of a minimum that was observed for VOTMPyP and MnTMPyP. The complicated LD^r and CD spectra observed at the highest R ratio (R = 0.14) suggested that the binding mode of CoTMPyP cannot be explained by a simple combination of monomeric outside binding and coupling of the porphyrins. Unlike the other porphyrins, CoTMPyP at R = 0.16 started to become aggregated. Thus, in the tested R ratio range, CoTMPyP conceivably binds to DNA with a binding mode that is a combination of monomeric outside binding, moderate stacking, in which the electric transition of a limited number of porphyrin molecules couple, and extensive stacking, which is a form of porphyrin assembly.

The directions of the changes in the absorption and CD spectra of TiOTMPyP with increasing R ratio appeared to be the same as those observed for VOTMPyP and MnTMPyP. However, the difference in the angle between the two electric transitions is slightly less, viz. only 3°, suggesting that the binding geometry of TiOTMPyP slightly deviated from those of VOTMPyP and MnTMPyP. A similar deviation was observed at the highest R ratio (R = 0.16). From these observations, the coupling between TiOTMPyP may be less efficient compared to VOTMPyP and MnTMPyP. VOTMPyP was suggested to form a hexa-coordinated VO(H_2O)TMPyP when associated with poly[d(A-T)$_2$] as well as in aqueous solution, whereas the sixth axial ligand was replaced by the component of the G base when associated with poly[d(G-C)$_2$].[52] In the complex formed with poly[d(G-C)$_2$], the amine group of the G base in the minor groove was proposed to be the sixth coordinated ligand of VOTMPyP.[54] These observations suggest that VOTMPyP is hexa-coordinated when it is associated with DNA or synthetic polynucleotides. The sixth axial ligand is H_2O at the AT base pairs, whereas it seems to be the amine group at the GC site.[43,45] A nonintercalative binding mode of VOTMPyP with AT sequence preference has been also reported.[59,70] Thus, the coordination number around the central metal complex conceivably is the reason for the less efficient electric transition coupling observed for TiOTMPyP. Co(II)TMPyP was stable when it binds to DNA or AT containing polynucleotides, whereas the oxidation state changed instantaneously to Co(III) in the presence of GC-rich polynucleotide,[49,50] supporting the ligation of the guanine N7 atom, which is known to be strong electron-donating ligands. Consequently, Co(III)TMPyP investigated in this study likely ligated with the guanine N7 amine when binds to GC base-pair, similarly with VOTMPyP.

Throughout this article, the term "outside binding" was used as the confrontation of the intercalation binding mode. A major groove binding mode that corresponds the "outside binding" was proposed for CoTMPyP based on combination of the magnetic CD spectrum and the binding angles measured by LD at a low [porphyrin]/[DNA base] ratio.[46] However, the magnetic CD spectrum indicated only a weak interaction between CoTMPyP and DNA. The angles of either 58 ± 1° or

42°, which were previously reported for the CoTMPyP−DNA complex,[45] were used as evidence for the major groove binding geometry. However, the former angle was obtained from the average LD^r value in the Soret region, whereas the latter was obtained from the assumption that the two electric transition moments were completely degenerate. Thus, neither of the previously reported angles reflects the true angle of the CoTMPyP−DNA complex, in which the degeneration of the two electric transitions was partially removed. Furthermore, it was reported that the spectral properties of CoTMPyP were similar when it was associated with the poly(dA)·poly(dT) duplex and the poly(dA)·[poly(dT)]$_2$ triplex.[55] The spectral properties of the CoTMPyP complexed with the poly(dG)·poly(dC) duplex were also similar to those of CoTMPyP complexed with the poly(dC)·poly(dG)·poly(dC) triplex. Considering that the third strand in the triplexes is located in the major groove of the template duplex, this observation provides strong evidence that CoTMPyP binds at the opposite side of the major groove, namely near the minor groove, in spite of a report in which major groove binding of CoTMPyP was proposed by a magnetic CD study.[46] Although an outside binding mode was suggested by a thermodynamic study in the MnTMPyP case,[71] three binding modes, namely modes 1, 2, and 3, corresponding to major groove binding, minor groove binding, and outside binding in the order of increasing [porphyrin]/[DNA base] ratio, were proposed by thorough analysis of CD spectra.[72] This suggestion is based on the observation that mode 1 was inhibited by the presence of methyl green, a major groove binding drug, and berenil, a known minor groove binder, inhibited modes 2 and 3. In mode 2, MnTMPyP was proposed to bind deep in the minor groove. However, the fact that measured CD and LD properties of the MnTMPyP−DNA complex are similar to those of the CoTMPyP−DNA complex (Figures 4 and 7) implies the binding mode of MnTMPyP resembles that of CoTMPyP. These observations are against the major groove binding mode of MnTMPyP for the reasons mentioned previously for CoTMPyP. The binding of methyl green at the major groove of DNA possibly induces the conformational change in the minor groove affecting indirectly the binding of MnTMPyP. Mode 2, binding deep in the minor groove,[72,73] in which the croissant type of side of the porphyrin molecule fits into the narrow groove, is also questionable because of the steric hindrance provided by the axial ligand. Furthermore, the binding angles of 45° and 90° for the B_x and B_y transition of porphyrin relative to the local DNA helix axis are expected from mode 2, which do not agree with measured angles for MnTMPyP (Table 1). All of this discussion indicates that the true nature of outside binding mode that is observed for MTMPyP with axial ligand(s) has not been fully clarified and requires further investigation.

CONCLUSION

In the intercalation pocket, the molecular plane of the planar porphyrins tilts to a large extent to each other. The DNA base plane also tilts with respect to the local DNA helix axis. The coupling of the electric transition moments can occur between the intercalated porphyrins separated by at least two base-pairs. The porphyrins with axial ligands exhibited the external binding mode, in which the tilt angle of one of the two electric transitions of the porphyrin is in the 56°∼59° range, whereas the other is in the range of 59°∼65° relative to the local DNA helix axis at low R ratios. As the electric coupling increases, the molecular plane of the porphyrin declines toward the helix axis. In the case of CoTMPyP, the binding mode was too complicated to analyze being a combination of monomeric outside binding and moderate stacking. Thus, extensive assembly may be involved.

AUTHOR INFORMATION

Corresponding Author

*Tel: +82 53 810 2362. Fax: +82 53 813 5412. E-mail: seogkim@yu.ac.kr.

Notes

The authors declare no competing financial interest.

ACKNOWLEDGMENTS

This study was supported by an internal research grant of Yeungnam University.

REFERENCES

(1) Pasternack, R. F.; Gibbs, E. J.; Villafranca, J. J. *Biochemistry* **1983**, *22*, 2406−2414.
(2) Fiel, R. J.; Howard, J. C.; Datta-Gupta, N. *Nucleic Acid Res.* **1979**, *6*, 3093−3118.
(3) Ding, L.; Balzarini, J.; Schols, D.; Meunier, B.; Clercq, E. *Biochem. Pharmacol.* **1992**, *44*, 1675−1679.
(4) Vicente, M. G. *Curr. Med. Chem. Anti-Cancer Agents* **2001**, *1*, 175−194.
(5) Zhao, P.; Xu, L.-C.; Huang, J.-W.; Zheng, K.-C.; Fu, B.; Yu, H.-C.; Ji, L.-N. *Biophys. Chem.* **2008**, *135*, 102−109.
(6) Zhao, P.; Xu, L.-C.; Huang, J.-W.; Zheng, K.-C.; Liu, J.; Yu, H.-C.; Ji, L. N. *Biophys. Chem.* **2008**, *134*, 72−83.
(7) Zhao, P.; Xu, L.-C.; Huang, J.-W.; Fu, B.; Yu, H.-C.; Zhang, W.-H.; Chen, J.; Yao, J.-H.; Ji, L. N. *Bioorg. Chem.* **2008**, *36*, 278−287.
(8) Robertson, C. A.; Evans, H. D.; Abrahamse, H. *J. Photochem. Photobiol. B.* **2009**, *96*, 1−8.
(9) Timothy, J.; Jensen, M.; Vicente, G. H.; Luguya, R.; Norton, J.; Fronczek, F. R.; Smith, K. M. *J. Photochem. Photobiol. B* **2010**, *100*, 100−111.
(10) de Oliveira Silva, F. R.; Bellini, M. H.; Nabeshima, C. T.; Schor, N.; Vieira, N. D., Jr; Courrol, L. C. *Photodiagn. Photodyn.* **2011**, *8*, 7−13.
(11) Guliaev, A. B.; Leontis, N. B. *Biochemistry* **1999**, *38*, 15425−15437.
(12) Lee, Y.-A.; Lee, S.; Cho, T.-S.; Kim, C.; Han, S. W.; Kim, S. K. *J. Phys. Chem. B.* **2002**, *106*, 11351−11355.
(13) Strickland, J. A.; Marzilli, L. G.; Wilson, W. D. *Biopolymers* **1990**, *29*, 1307−1323.
(14) Kuroda, R.; Tanaka., H. J. *Chem. Soc. Chem. Commun.* **1994**, 1575−1576.
(15) Schneider, H. -J.; Wang, M. *J. Org. Chem.* **1994**, *59*, 7473−7478.
(16) Pasternack, R. F.; Goldsmith, J. I.; Gibbs, E. J. *Biophys. J.* **1998**, *75*, 1024−1031.
(17) Yun, B. H.; Jeon, S. H.; Cho, T.-S.; Yi, S. Y.; Sehlstedt, U.; Kim, S. K. *Biophys. Chem.* **1998**, *70*, 1−10.
(18) Lee, S.; Jeon, S. H.; Kim, B. -J.; Han, S. W.; Jang, H. G.; Kim, S. K. *Biophys. Chem.* **2001**, *92*, 35−45.
(19) Park, T.; Kim, J. M.; Han, S. W.; Lee, D. -J.; Kim, S. K. *Biochim. Biophys. Acta* **2005**, *1726*, 287−292.
(20) Carvlin, M. J.; Datta-Gupta, N.; Fiel, J. *Biophys. Res. Commun.* **1982**, *108*, 66−73.
(21) Carvlin, M. J.; Fiel, R. J. *Nucleic Acids Res.* **1983**, *11*, 6121−6139.
(22) Banville, D. L.; Marzilli, L. G.; Strickland, J. A.; Wilson, W. D. *Biopolymers* **1986**, *25*, 1837−1858.
(23) Mukundan, N. E.; Pethö, G.; Dixon, D. W.; Marzilli, L. G. *Inorg. Chem.* **1995**, *34*, 3677−3687.
(24) Mallamace, F.; Micali, N.; Monsu'Scolaro, L.; Pasternack, R. F.; Romeo, A.; Terracina, A.; Trusso, S. J. *J. Mol. Struct.* **1996**, *383*, 255−260.

(25) Pasternack, R. F.; Gibbs, E. J.; Collings, P. J.; de Paula, J. C.; Turzo, L. C.; Terracina, A. *J. Am. Chem. Soc.* **1998**, *120*, 5873−5878.
(26) Pasternack, R. F.; Gibbs, E. J.; Bruzewicz, D.; Stewart, D.; Engstrom, K. S. *J. Am. Chem. Soc.* **2002**, *124*, 3533−3539.
(27) Pasternack, R. F. *Chirality* **2003**, *15*, 329−332.
(28) Scolaro, L. M.; Romeo, A.; Pasternack, R. F. *J. Am. Chem. Soc.* **2004**, *126*, 7178−7179.
(29) Lee, Y.-A.; Kim, J.-O.; Cho, T.-S.; Song, R.; Kim, S. K. *J. Am. Chem. Soc.* **2003**, *125*, 8106−8107.
(30) Kim, J.-O.; Lee, Y.-A.; Yun, B. H.; Han, S. W.; Kwaq, S. T.; Kim, S. K. *Biophys. J.* **2004**, *86*, 1012−1017.
(31) Park, T.; Shin, J. S.; Han, S. W.; Son, J.-K.; Kim, S. K. *J. Phys. Chem. B.* **2004**, *108*, 17106−17111.
(32) Kelly, J. M.; Murphy, M. J.; McConnell, D. J.; PhGuigin, C. *Nucleic Acids Res.* **1985**, *13*, 167−184.
(33) Marzilli, L. G.; Banville, D. L.; Zon, G.; Wilson, W. D. *J. Am. Chem. Soc.* **1986**, *108*, 4188−4192.
(34) Gibbs, E. J.; Maurer, M. C.; Zhang, J. H.; Reiff, W. M.; Hill, D. T.; Malicka-Blaszkiewicz, M.; McKinnie, R. E.; Liu, H.-Q.; Pasternack, R. F. *J. Inorg. Biochem.* **1988**, *32*, 39−65.
(35) Fiel, R. J. *J. Biomol. Struct. Dyn.* **1989**, *6*, 1259−1275.
(36) Jin, B.; Lee, H. M.; Lee, Y.-A.; Ko, J. H.; Kim, C.; Kim, S. K. *J. Am. Chem. Soc.* **2005**, *127*, 2417−2424.
(37) Chae, Y.-H.; Jin, B.; Kim, J.-K.; Han, S. W.; Kim, S. K.; Lee, H. M. *Bull. Korean Chem. Soc.* **2007**, *28*, 2203−2208.
(38) Ward, B.; Skorobogaty, A.; Dabrowiak, J. C. *Biochemistry* **1986**, *25*, 6875−6883.
(39) Geacintov, N. E.; Ibanez, V.; Rougee, M.; Bensasson, R. V. *Biochemistry* **1987**, *26*, 3087−3092.
(40) Strickland, J. A.; Marzilli, L. G.; Gay, K. M.; Wilson, W. D. *Biochemistry* **1998**, *27*, 8870−8878.
(41) Bütje, K.; Cshneider, J. H.; Kim, J.-J. P.; Wang, Y.; Ikuta, S.; Nakamoto, K. *J. Inorg. Biochem.* **1989**, *37*, 119−134.
(42) Sari, M. A.; Battioni, J. P.; Dupré, D.; Mansuy, D.; Le Pecq, J. B. *Biochemistry* **1990**, *29*, 4205−4215.
(43) Bütje, K.; Nakamoto, K. *J. Inorg. Biochem.* **1990**, *39*, 75−92.
(44) Dougherty, G.; Pasternack, R. F. *Biophys. Chem.* **1992**, *44*, 11−19.
(45) Sehlstedt, U.; Kim, S. K.; Carter, P.; Soodisman, J.; Vollano, J. F.; Nordén, B.; Dabrowiak, J. C. *Biochemistry* **1994**, *33*, 417−426.
(46) Barnes, N. R.; Schreiner, A. F. *Inorg. Biochem.* **1998**, *37*, 6935−6938.
(47) Batinić-Haberle, I.; Benov, L.; Spasojević, I.; Fridovich, I. *J. Biol. Chem.* **1998**, *273*, 24521−24528.
(48) Trommel, J. S.; Marzilli, L. G. *Inorg. Chem.* **2001**, *40*, 4374−4383.
(49) Terekhov, S. N.; Kruglik, S. G.; Malinovskii, V. L.; Galievsky, V. A.; Chirvony, V. S.; Turpin, P.-V. *J. Raman Spectrosc.* **2003**, *34*, 868−881.
(50) Terekhov, S. N.; Galievsky, V. A.; Chirvony, V. S.; Turpin, P.-V. *J. Raman Spectrosc.* **2005**, *36*, 962−973.
(51) Nyarko, E.; Hanada, N.; Habib, A.; Tabata, M. *Inorg. Chim. Acta* **2004**, *357*, 739−745.
(52) Cho, D. W.; Jeong, D. H.; Ko, J. H.; Kim, S. K.; Yoon, M. *J. Photochem. Photobiol. A, Chem.* **2005**, *174*, 207−313.
(53) Lee, M. J.; Lee, G.-J.; Lee, D.-J.; Kim, S. K.; Kim, J.-M. *Bull. Korean Chem. Soc.* **2005**, *26*, 1728−1734.
(54) Park, T. G.; Ko, J. H.; Ryoo, A. Y.; Kim, J.-M.; Cho, D. W.; Kim, S. K. *Biochem. Biophys. Acta* **2006**, *1760*, 388−394.
(55) Jin, B.; Shin, J. S.; Bae, C. H.; Kim, J.-M; Kim, S. K. *Biochem. Biophys. Acta* **2006**, *1760*, 993−1000.
(56) Kim, Y. R.; Gong, L.; Park, J.; Jang, Y. J.; Kim, J.; Kim, S. K. *J. Phys. Chem. B.* **2012**, *116*, 2330−2337.
(57) Rebouças, J. S.; Spasojević, I.; Batinić-Haberle, I. *J. Pharm. Biomed. Anal.* **2008**, *48*, 1046−1049.
(58) Lu, M.; Guo, Q.; Pasternack, R. F.; Wink, D. J.; Seeman, N. C.; Kallenbach, N. R. *Biochemistry* **1990**, *29*, 1614−1624.
(59) Lin, M.; Lee, M.; Yue, K. T.; Marzilli, L. G. *Inorg. Chem.* **1993**, *32*, 3217−3226.
(60) Harriman, A.; Porter, G. *J. Chem. Soc., Faraday Trans. II* **1979**, 1532−1542.
(61) Ismail, M. A.; Rodger, P. M.; Rodger, A. *J. Biomol. Struct. Dyn.* **2000**, *11*, 335-348.
(62) Nordén, B.; Kubista, M.; Kurucsev, T. *Q. Rev. Biophys.* **1992**, *25*, 51−170.
(63) Rodger, A.; Nordén, B. *Circular Dichroism and Linear Dichroism*; Oxford University Press, New York, 1997.
(64) Nordén, B.; Seth, S. *Appl. Spectrosc.* **1985**, *39*, 647−655.
(65) Gandini, S. C.; Yushmanov, V. E.; Perussi, J. R.; Tabak, M.; Borissevitch, I. E. *J. Inorg. Biochem.* **1999**, *73*, 35−40.
(66) Lee, S.; Lee, Y.-A.; Lee, H. M.; Lee, J. Y.; Kim, D. H.; Kim, S. K. *Biophys. J.* **2002**, *83*, 371−381.
(67) Nonaka, Y.; Lu, D. S.; Dwivedi, A.; Strommen, D. P.; Nakamoto, K. *Biopolymers* **1990**, *29*, 999−1004.
(68) Galievsky, V. A.; Chirvony, V. S. *J. Phys. Chem.* **1996**, *100*, 12649−12659.
(69) Wheeler, G.; Miskovsky, P.; Jancura, D.; Chinsky, L. *J. Biomol. Struct. Dyn.* **1998**, *15*, 967−985.
(70) Strickland, J. A.; Marzilli, L. G.; Gay, K. M.; Wilson, W. D. *Biochemistry* **1988**, *27*, 8870−8878.
(71) Dezhampanah, H.; Bordbar, A.-K.; Tangestaninejad, S. *J. Porphyrins Phthalocyanines* **2009**, *13*, 964−972.
(72) Nitta, Y.; Kuroda, R. *Biopolymers* **2006**, *81*, 376−391.
(73) Romera, C.; Sabater, L.; Garofalo, A.; Doxon, I. M.; Pratviel, G. *Inorg. Chem.* **2010**, *49*, 8558−8567.